The Curse of Numerical Noise and Implications for CFD-Based Design Optimization

Carl A. Gilkeson*
Institute of Thermofluids, School of Mechanical Engineering, University of Leeds, Leeds, LS2 9JT, UK

Vassili V. Toropov†
School of Engineering and Materials Science, Queen Mary University of London, London E1 4NS,UK

Harvey M. Thompson‡, Mark C. T. Wilson§
Institute of Thermofluids, School of Mechanical Engineering, University of Leeds, Leeds, LS2 9JT, UK

Natalie A. Foxley**
School of Computing, University of Leeds, Leeds, LS2 9JT, UK

Philip H. Gaskell††
School of Engineering and Computing Sciences, Durham University, South Road, Durham DH1 3LE, UK

Numerical noise is an unavoidable by-product of Computational Fluid Dynamics (CFD) simulations which, in the context of design optimization, may lead to challenges in finding optimum designs. This article draws attention to this issue by illustrating the difficulties it can cause for road vehicle aerodynamics simulations.

Firstly, a benchmark problem, flow past the Ahmed body, is used to highlight the effect of numerical noise on the calculation of aerodynamic drag. A series of simulations are conducted using three commonly employed Reynolds-Averaged Navier-Stokes (RANS) based turbulence models. Noise amplitudes of up to 22% are evident and the level of noise depends on the combination of turbulence model and grid used. Overall the Spalart Allmaras model is shown to be the least susceptible to noise levels for this particular application.

Secondly, multi-objective aerodynamic shape optimization is applied to a low-drag aerodynamic fairing for a livestock trailer. The fairing is parameterised in terms of three design variables. Moving Least Squares (MLS) metamodels are constructed from 50 high-fidelity CFD solutions for two objective functions. Subsequent optimization is successful for the first objective, however numerical noise levels in excess of 7% are found to be problematic for the second one. A deliberate revision to the problem reduces the amount of noise present and leads to success with the construction of a small Pareto Front. Further analysis underlines the inherent capability of MLS metamodels in dealing with noisy CFD responses. Suggestions are also made to improve the chances of success for future investigations.

Nomenclature

$A_{3\sigma}$	=	Percentage amplitude of noise
C_D	=	Aerodynamic drag coefficient
d_i	=	i^{th} design variable
f_r	=	Noise oscillation frequency
F_1	=	Objective function for aerodynamic drag
F_2	=	Objective function for ventilation rate

Communicating Author: C.A.Gilkeson@leeds.ac.uk
* Teaching & Research Fellow in Aeronautical and Aerospace Engineering.
† Professor of Aerospace Engineering.
‡ Professor of Computational Fluid Dynamics.
§ Lecturer of Mechanical Engineering
** PhD Candidate
†† Professor of Fluid Mechanics

F_3 = Objective function for temperature humidity index
Ψ = Rear slant angle of Ahmed body
Ω = Noise oscillation parameter
σ = One standard deviation
CFD = Computational Fluid Dynamics
DoE = Design of Experiments
MLS = Moving Least Squares
RANS = Reynolds-Averaged Navier-Stokes
THI = Temperature humidity index

I. Introduction

THE speed and power of computers has increased dramatically in recent years with performance improvements estimated to be between 1000 and 10,000 times compared to 20 years ago[1]. This capability is being exploited in the field of Computational Fluid Dynamics (CFD)-based optimization which is being harnessed across a range of areas including aerospace engineering[2,3], tribology[4], polymer moulding[5], ship design[6], vehicle aerodynamics[7-10], hospital ward ventilation[11] and jet pump design[12]. While these examples demonstrate the versatility of CFD-based optimization, there is one aspect which can prove problematic: the presence of numerical noise in the CFD responses[10,13-19].

Numerical noise has long been a hindrance for computation with problems first reported from finite element tidal simulations in 1974[20] as well as other related examples in the subsequent years[21-23]. In these cases, numerically induced oscillations were particularly troublesome. To the authors' knowledge, the investigation by Giunta et al.[13] is the first to cite numerical noise as a hindrance to numerical optimization in the design of a high-speed civil airliner using CFD. Optimization on polynomial response surfaces was made difficult by spurious noise-induced local minima, which 'trapped' the optimizer. Implementing a method of skipping over these local minima using large move limits in the initial stages of the optimization search was beneficial, however this approach did not address the fundamental problem and no single optimum solution was found.

Later the impact of noise on response surfaces was also discussed by van Keulen et al.[14] for structural applications. Madsen et al.[15] and Shyy et al.[16] commented that noise originating from numerical simulations is much less recognised than for physical experiments. It is important to appreciate that numerical noise is an inherent by-product of computer simulation[15,24,25] which cannot be avoided. Furthermore, the observed behaviour is rather different from the noisy responses originating from experiments. For a given physical experiment there will be statistical variation in the answer due to errors and uncertainties originating from controlled and uncontrolled variables. In contrast, numerical experiments produce the same output for a given set of input variables provided all aspects of the simulation are constant (e.g. matching initial/boundary conditions, identical grid structure, solver version and computer hardware/architecture). What distinguishes numerical experiments from their physical counterparts is that the errors (and thus the noise) are repeatable due to their deterministic nature[18].

It follows that for optimization studies requiring analysis of a wide range of designs (e.g. via metamodelling) this characteristic can lead to problems in identifying optimum designs[10,13]. Whilst these issues have received attention there are no studies dedicated exclusively to numerical noise and the negative impact it can have on CFD-based optimization. The purpose of this article is to draw attention to these in the context of road vehicle aerodynamics. It is structured as follows: Section II characterizes numerical noise for a benchmark vehicle aerodynamics problem. Section III describes an investigation into aerodynamic shape optimization of a low-drag fairing for a practical road vehicle, where the difficulty of metamodel-based optimization in the face of noisy CFD responses is highlighted. Finally sections IV and V draw on the results from sections II and III to propose strategies for dealing with numerical noise in the context of CFD-based design optimization.

II. Numerical Noise: Analysis of the Ahmed body

The Ahmed body is a simple generic road vehicle commonly used as a benchmark for vehicle aerodynamics. Ahmed[26] conducted a wind tunnel investigation around this shape and the results are often used to validate numerical simulations. This section describes numerical results obtained for the flow around the Ahmed body with emphasis on numerical noise.

A. Ahmed body

Fig. 1 illustrates the Ahmed body which consists of a solid block measuring 0.94 m long, 0.39 m wide and 0.29 m high. It has rounded leading edges with a radius of 0.10 m at the front and a notch rear with a slanted face. The size of the notch is governed by the slant angle, ψ, which is kept constant at 30°. In order to simulate the flow field around the vehicle, a solid model was generated using Ansys Design Modeler (version 13.0)[27].

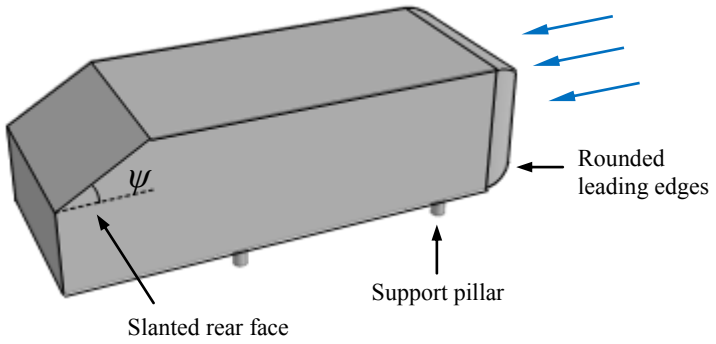

Figure 1: The Ahmed body

The size and shape of the air volume surrounding the vehicle is defined using the dimensions of the wind tunnel originally used by Ahmed[26]. The closed-return open working section tunnel was supplied with airflow through a square nozzle of 3 m x 3 m. The vehicle was mounted on a ground board of length 5 m with the vehicle centre located 2.13 m downstream of the inlet. To reduce the computational effort a symmetry plane was employed and the working section was assumed to have a constant cross-section matching the dimensions of the inlet nozzle. No-slip boundary conditions were used on all solid walls, whereas the side and ceiling of the domain were assigned a zero shear stress boundary condition which is appropriate given the original open-section wind tunnel layout.

B. Numerical grid structure

Recent CFD investigations of airflow past a bluff vehicle in a wind tunnel have demonstrated the importance of grid density, cell type and the choice of turbulence model for predicting aerodynamic drag[28,29]. In this investigation three grid densities are considered for each of the following cell types: (i) hexahedral, (ii) tetrahedral and (iii) polyhedral, giving 9 grids in all. Each of these employ a boundary layer grid adjacent to solid walls, see Fig. 2.

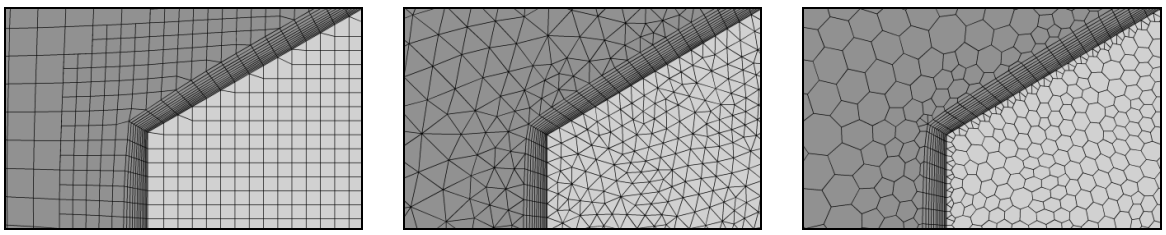

(a) (b) (c)

Figure 2: Local grid structure on the symmetry plane (dark cells) at the rear of the Ahmed body for (a) hexahedral, (b) tetrahedral and (c) polyhedral cell types.

Table 1 summarises each grid and Fig. 2 shows the local grid structure at the base of the vehicle for the coarse hexahedral, tetrahedral and polyhedral grids respectively. The hexahedral and tetrahedral grids were generated with AnsysMesh (version 13.0)[27] and the polyhedral grids were produced using an agglomeration procedure within Fluent (version 13.0.0-sp2)[27] which converts a standard tetrahedral grid into an equivalent polyhedral one.

		Global Cell Count		
Grid type	Local grid spacing (m)	Hexahedral	Tetrahedral	Polyhedral
Coarse	0.015	229512	396106	173934
Medium	0.010	479865	703887	302074
Fine	0.007	699314	1383917	583475

Table 1: Grid statistics

C. Turbulence models

The choice of turbulence model is an important consideration prior to computing solutions to the governing incompressible Navier-Stokes equations. This is especially so for high Reynolds number turbulent flow such as the one being investigated. In order to assess the impact of turbulence model on the amount of numerical noise present, three models suitable for simulating external aerodynamics, were chosen, namely: (i) the Spalart Allmaras model[30] (SA), (ii) the realizable k-ε model[31] (RKE) and (iii) Menter's shear-stress-transport k-ω model[32] (SSTKO).

Steady-state solutions were computed using Fluent (version 13.0.0-sp2)[27] for each turbulence model on all 9 grids, giving 27 solutions in total. All solutions assumed a free-stream velocity of 60 m/s and turbulence intensity of 0.5% at the inlet[26] (Note that the relatively high inlet velocity is to compensate for the reduced scale of the vehicle, leading to a Reynolds Number of 4.3 million which is consistent with the original experiments[26]). Irrespective of the turbulence model-grid combination employed, every simulation utilised second order discretisation of the flow equations in conjunction with the SIMPLE[33] pressure-velocity coupling algorithm. Although solution convergence was generally achieved in fewer than 1000 iterations, all simulations were run for a total of 5000 iterations to eliminate convergence errors.

D. Quantification of numerical noise

For each of the simulations described above, the drag coefficient of the vehicle, C_D, was monitored throughout the 5000 iteration cycle. In all cases numerical noise was evident, characterised by a combination of structured periodic cycles with apparently random oscillations superimposed. Fig. 3 shows a typical noise sample from one of the simulations, taken from iterations beyond the point of solution convergence.

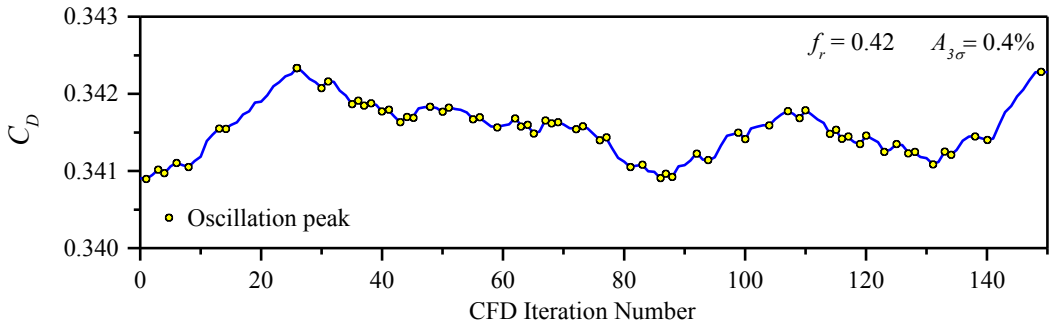

Figure 3: Example of numerical noise shown by one SA solution on the fine hexahedral grid.

Interpretation of these characteristics is difficult from visual inspection alone and so there is a need to quantify the noise levels more precisely. The noise levels can be decomposed into the frequency and the amplitude of oscillation. The former is conveniently defined by the percentage oscillation frequency, f_r, given by:

$$f_r = 100 \frac{\sum_{i=0}^{n} \Omega_i}{n}, \tag{1}$$

where Ω_i is the oscillation parameter evaluated for the i^{th} iteration for a sample size of n iterations. For a monotonic increase in C_D from one iteration to the next, $\Omega = 0$. For a maximum or minimum point (i.e. oscillation peak in Figure 3) the sign of the gradient dC_D/di changes and so $\Omega = 1$. Therefore, if $f_r = 0$ the signal is likely to be stable with no oscillations present, whereas $f_r = 100$ is indicative of a fully oscillatory signal where the gradient changes sign every iteration. A point of note is that f_r accounts for all local gradient changes but it does not consider low-frequency oscillations (e.g. on the order of 100's of iterations). As CFD solutions for steady state problems are typically taken from the final iteration, low-frequency oscillations are far less influential and thus less relevant than the high frequency ones described by f_r.

As well as frequency, the amplitude of each individual oscillation is important as it accounts for the *magnitude* of the variations. For a given sample size, three standard deviations, 3σ, is an adequate measure of the data spread because it accounts for 99.7% of the values recorded. This is used to define the percentage amplitude of noise, $A_{3\sigma}$, (for the sample) relative to the mean value, namely:

$$A_{3\sigma} = 100 \frac{3 \cdot \sigma}{\overline{C_D}}, \tag{2}$$

where σ is the standard deviation and $\overline{C_D}$ is the mean drag coefficient for a sample of size n. As with f_r, small values of $A_{3\sigma}$ signify less noise whereas larger ones signify a noisy response. For the 150-iteration sample shown in Fig. 3, f_r = 42.0% and $A_{3\sigma}$ = 0.4%; i.e. the noise is frequent but its impact is minimal because of the small amplitude.

E. Impact of grid type, cell type and turbulence model

The parameters defined by equations (1) and (2) are used to analyse the numerical noise present in the data obtained for C_D for the range of iterations: 2500-5000, per simulation. A sensitivity study showed that this sample size is large enough to adequately characterise both f_r and $A_{3\sigma}$ and it only considers the converged region of each solution. Table 2 summarises these parameters along with the mean drag coefficient, $\overline{C_D}$, for the range of grid-turbulence model combinations tested. In all cases the computed drag coefficients are less than the equivalent experimental value[26] of 0.378. Overall the SA model gives the most satisfactory result with the RKE and SSTKO models generally exhibiting the smallest drag values.

		SA			RKE			SSTKO		
Grid type	Cell type	$\overline{C_D}$	f_r (%)	$A_{3\sigma}$ (%)	$\overline{C_D}$	f_r (%)	$A_{3\sigma}$ (%)	$\overline{C_D}$	f_r (%)	$A_{3\sigma}$ (%)
Coarse	Hexahedral	0.368	55.7	0.1	0.339	79.1	0.1	0.309	14.5	1.6
Medium	Hexahedral	0.353	8.6	0.2	0.313	13.8	0.0	0.298	24.0	1.1
Fine	Hexahedral	0.341	39.2	0.4	0.342	41.4	0.5	0.300	13.2	1.6
Coarse	Tetrahedral	0.367	95.1	0.4	0.377	9.4	22.6	0.324	28.0	7.6
Medium	Tetrahedral	0.354	100.0	0.0	0.308	16.3	2.3	0.304	39.8	0.0
Fine	Tetrahedral	0.351	96.2	0.8	0.317	75.2	8.3	0.332	76.4	7.2
Coarse	Polyhedral	0.354	100.0	0.0	0.318	49.8	0.0	0.327	100.0	0.0
Medium	Polyhedral	0.346	2.6	0.1	0.302	39.8	0.0	0.309	9.2	5.1
Fine	Polyhedral	0.344	3.2	0.3	0.296	23.0	0.1	0.299	13.6	3.2

Table 2: Computed mean drag coefficients and associated numerical noise as a function of grid type, cell type and turbulence model. Note: from ref 26 the experimental drag coefficient, $C_D = 0.378$.

Both f_r *and* $A_{3\sigma}$ vary considerably, depending on the grid and cell type and the turbulence model; clearly all three factors impact the noise levels which is consistent with earlier studies[15-17]. The differences in the observed values of f_r illustrate that the noise levels are not in phase from one simulation to another. In terms of the amplitude of oscillations they are below 1% for all SA solutions, however variations as high as 22.6% and 7.6% are present in the solutions for the RKE and SSTKO models, respectively. The choice of turbulence model is instrumental in determining the noise levels for this particular application.

In many cases the frequency and the amplitude are greatest for solutions computed on the tetrahedral grids compared to the hexahedral and polyhedral ones, however there is no apparent correlation with the grid density. In some cases the noise amplitude increases as the grid becomes finer, e.g. SA solutions on the hexahedral and polyhedral grids. However, for the remaining cases the largest amplitudes (per combination of cell type and turbulence model) can occur for either the coarse, medium or fine grid densities. Whilst there is a lack of generality for these results, the fine-grid solutions are inevitably closer to being grid independent and so these are more relevant to the overall discussion.

Fig. 4 shows a 400-iteration sample of the relative drag coefficient (with respect to the mean value, $\overline{C_D}$) as a function of turbulence model and cell type for fine-grid solutions only. For all cases the noise levels exhibited by the tetrahedral-grid solutions are noticably greater than the equivalent hexahedral and polyhedral ones with multi-modal responses clearly seen. Solutions obtained on the hexahedral and polyhedral grids show noise levels with significantly smaller amplitudes and reduced frequencies. Considering the results for each turbulence model in turn, the noise levels are smallest for the SA model with a range of values generally within ±0.5% of the mean with the exception of some local variations of the order ±1.0% for the tetrahedral-grid solutions, see Fig. 4(a). For the RKE model, again both the hexahedral and polyhedral grid solutions show variations within ±0.5% of the mean value, however those for the tetrahedral grid are up to ±8.0%, Figure 4(b). The same trend is seen for the SSTKO model although the hexahedral and polyhedral-grid solutions exhibit larger variations of ±3.0% compared to those obtained with the other models. In summary, these results illustrate the extent of

numerical noise for what is a relatively simple application. This striking variation of output is also seen in more complicated flow problems as will be shown in the following section.

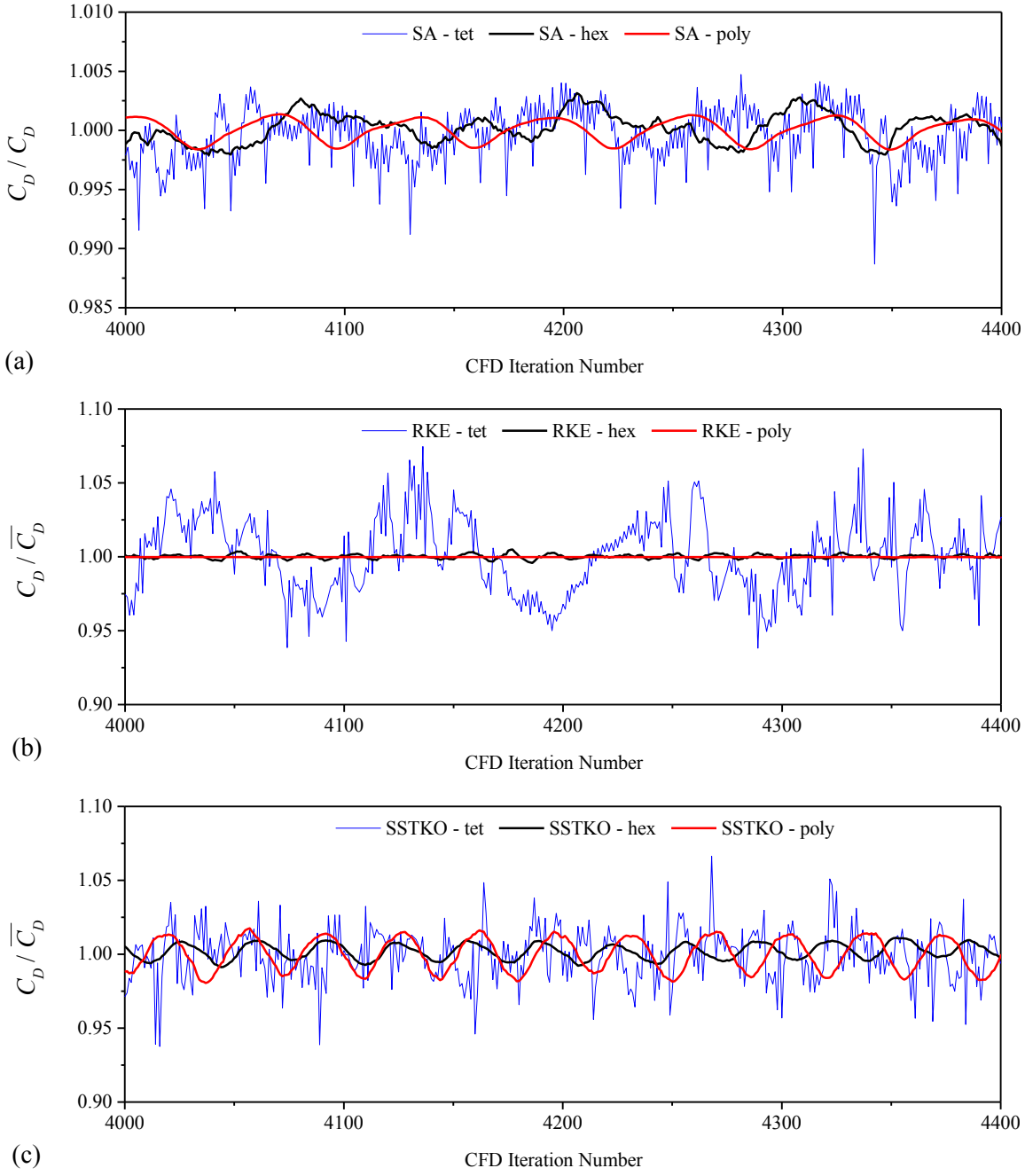

Figure 4: Plots of the relative drag coefficient ($C_D / \overline{C_D}$) as a function of steady-state iteration number per grid cell type for (a) SA, (b) RKE and (c) SSTKO turbulence models. Note the smaller y-axis scale for (a).

III. CFD-Based Optimization

The results presented above demonstrate how a very basic parameter, the drag coefficient, can vary substantially in steady-state CFD simulations. Cleary this has implications for CFD-based design optimization methods because many designs are typically evaluated with each being susceptible to varying levels of noise. The following section considers the effect this can have as part of an optimization problem for a practical engineering investigation.

A. Livestock trailer design

The majority of animals transported between farms, abattoirs, and markets within the United Kingdom are carried in small box-shaped livestock trailers, such as the one depicted in Fig. 5. They are towed by off-road vehicles and ventilation is supplied passively by virtue of vehicle movement. A series of rectangular side vents allow for air exchange between the internal environment and the external free-stream. This is effective at maintaining a stable micro-environment in the upper deck, however the lower deck exhibits reduced ventilation[28,29].

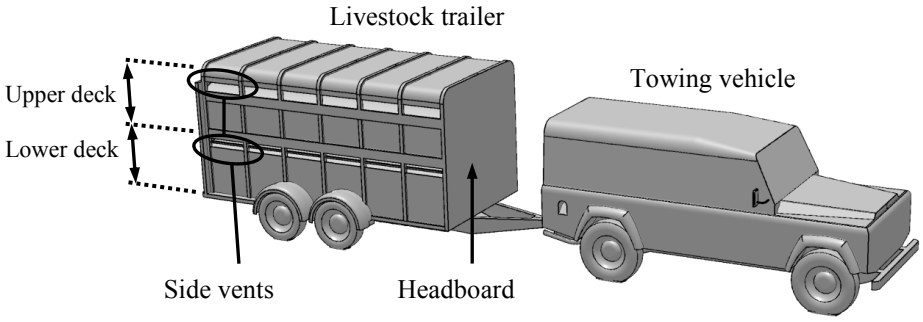

Figure 5: Illustration of a typical livestock trailer and towing vehicle.

B. Optimization problem formulation and design of experiments

Implementing changes to the trailer layout to improve the conditions in the lower deck is not viable due to practical constraints, however, implementing a retrofitted headboard fairing represents a feasible solution; with the purpose being to (i) reduce aerodynamic drag whilst (ii) maximising ventilation within the trailer. Such a problem lends itself to multi-objective metamodel-based optimization and this is the approach used here.

The proposed fairing is parameterised in terms of three design variables, namely the side radius, d_1, the lower edge extension, d_2 and the central extension of the fairing, d_3, see Figs. 6a and 6b. The purpose is to apply aerodynamic shape optimization in satisfying the following criteria:

$$\min F_1(\boldsymbol{d}) \text{ and } \max F_2(\boldsymbol{d}), \tag{3}$$

where

$$d_i^L \le d_i \le d_i^U,\ i = 1, 2, 3; \tag{4}$$

F_1 and F_2 are the objective functions for the aerodynamic drag coefficient (dimensionless) and the ventilation rate (m^3/s), respectively while d_i is the i^{th} design variable subject to relevant lower (d_i^L) and upper (d_i^U) physical constraints.

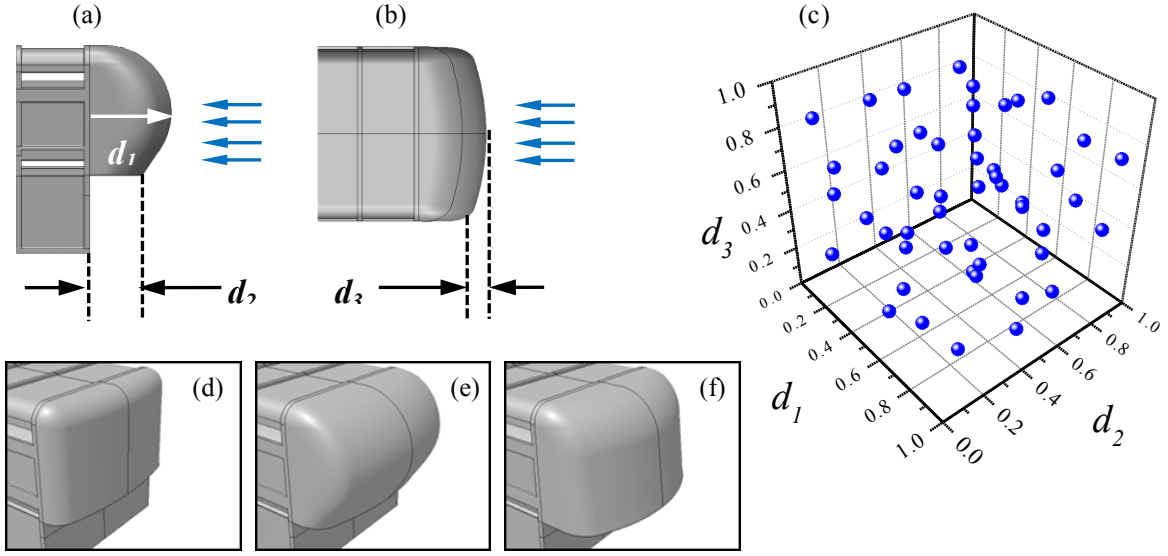

Figure 6: Parameterisation of the headboard fairing viewed from (a) the side and (b) above the trailer, (c) plot of the Design of Experiments (DoE) together with three sample fairing designs (d-f).

The optimization strategy involves building metamodels for each objective function (F_1 and F_2) and then optimizing on these to obtain a Pareto front from which to determine the optimum fairing design. To achieve this, each metamodel is fitted to CFD responses from fifty fairing designs which are chosen by an Optimal Latin Hypercube (OLH) Design of Experiments (DoE)[34]. Fig. 6(c) depicts the DoE and three sample fairings, Figs. 6(d-f), which exist within the design space. In important characteristics of the DoE is the uniformity of point coverage which is governed by the Audze-Eglais potential energy criterion[35,36].

C. CFD Solutions

Steady-state CFD solutions to the governing incompressible Navier-Stokes equations were used to assess each fairing by obtaining values of F_1 and F_2. A preliminary grid independence study carried out on the baseline trailer (Fig. 5) showed that a hybrid hexahedral-tetrahedral grid consisting of 6.7 million cells led to small discretisation errors of 1.5% and 2.0% for F_1 and F_2, respectively[10.] As demonstrated in section II, solutions computed on both hexahedral and polyhedral cell types lead to reduced noise levels compared to tetrahedral cells. In practice, hexahedra are easier to implement than polyhedra and they are less susceptible to numerical diffusion. For this reason hexahedral cells were placed in as many regions of the solution domain as possible including a structured boundary layer grid adjacent to the primary surfaces of the livestock trailer. Inevitably tetrahedral cells were required in the remaining volume due to the geometric complexity which illustrates one of the challenges of practical CFD application.

As shown previously, the Spalart Allmaras turbulence model generally exhibits small noise amplitudes for road vehicle aerodynamics simulations. Preliminary simulations of flow around the baseline configuration (Figure 5) verified that this model performs better than both the SSTKO and RKE models. Furthermore, the SA model has been shown to produce accurate results when validated against wind tunnel experiments of a $1/7^{th}$ scale livestock trailer[28]. Computations were carried out using Fluent[27] (version 6.3) for a total of 10,000 iterations and convergence of all quantities was observed after 9000 of these, thus ensuring that no inaccuracies were present due to convergence error.

D. Optimization strategy

Having obtained all fifty sets of CFD solutions, metamodels were built for each objective function using the Moving Least Squares (MLS) method[37,38] within HyperStudy (version 8)[39]. This technique caters for noisy responses by selecting an appropriate closeness of fit parameter, θ, which is contained within a Gaussian weight decay function, namely:

$$w_j = \exp\left(-\theta r_j^2\right), \tag{5}$$

where r_j is the Euclidean distance of the metamodel prediction location from the j^{th} DoE point[38]. High noise-smoothing is achieved if θ is small because the fit is loose due to the approximation whereas high values of θ lead to interpolation and no smoothing. Each metamodel was tuned to give the optimum value of θ to ensure the best fit to the CFD responses, see ref 10 for more details.

Once constructed, each MLS metamodel was analysed with a combination of global and local search methods using a Genetic Algorithm (GA) and the Sequential Quadratic Programming (SQP) technique, respectively. This strategy was used to locate candidates for an optimum design (per metamodel) before validating with a CFD solution and repeating the process until an optimum design was converged upon.

E. Numerical noise issues

For each CFD simulation, responses for F_1 or F_2 were taken from the final iteration. Satisfying the second objective of maximising ventilation proved difficult because all fifty fairing designs resulted in poorer ventilation compared to the baseline case (i.e. no fairing present). Further analysis showed that the presence of any given fairing streamlined the front of the trailer which guided airflow past the vents instead of through them thereby reducing the ventilation rate. Consequently, maximizing ventilation (equation 3) is not feasible with the current problem formulation. Instead, the second objective was changed such that the percentage reduction in ventilation rate could be minimized (min $F_2(\boldsymbol{d})$) which is equivalent to minimising the negative impact that the fairing has on ventilation[10].

The optimization strategy described above was applied to both objectives. The first objective, to minimise drag, was achieved at the expense of only one extra simulation which used a parameter set from one corner of the design space. In contrast, the second objective of minimising the reduction in ventilation rate was unsuccessful: the optimizer repeatedly predicted a fairing which was poorer than many of the DoE points. Despite this the proposed design was evaluated using an additional CFD simulation but this made no change and the design exhibited poor performance. In an effort to construct a Pareto front with the possibility of finding better ventilation designs, four additional designs were suggested by the metamodel. Each of these was found by placing a constraint on F_1 to give F_2 for each design[10]. CFD solutions were obtained for each but the results were poor and they did not lead to an optimum design for this objective.

The presence of numerical noise in each CFD solution for F_2 was suspected to be the cause of the difficulties encountered. This is explored in Fig. 7 which shows a typical solution history where the drag coefficient, C_D, and the ventilation rate, Q, are plotted as a function of the iteration number. Note that C_D and Q are the basis for F_1 and F_2 respectively. Closer inspection of C_D over the converged portion of the data (Fig. 7b) shows that the noise frequency is relatively high at 36.7%, although this is accompanied by a small amplitude of 0.6% (i.e. ± 0.3%). In contrast, Q, which is used in the calculation of F_2, exhibits lower frequency noise of 1.3%, however, the amplitude is large at 7.0%.

In light of these noise levels, it is unsurprising that the optimization of F_2 was unsuccessful. Each CFD solution was taken from the final (10,000th) iteration which could have coincided with any point on the noisy response which was independent of the design.

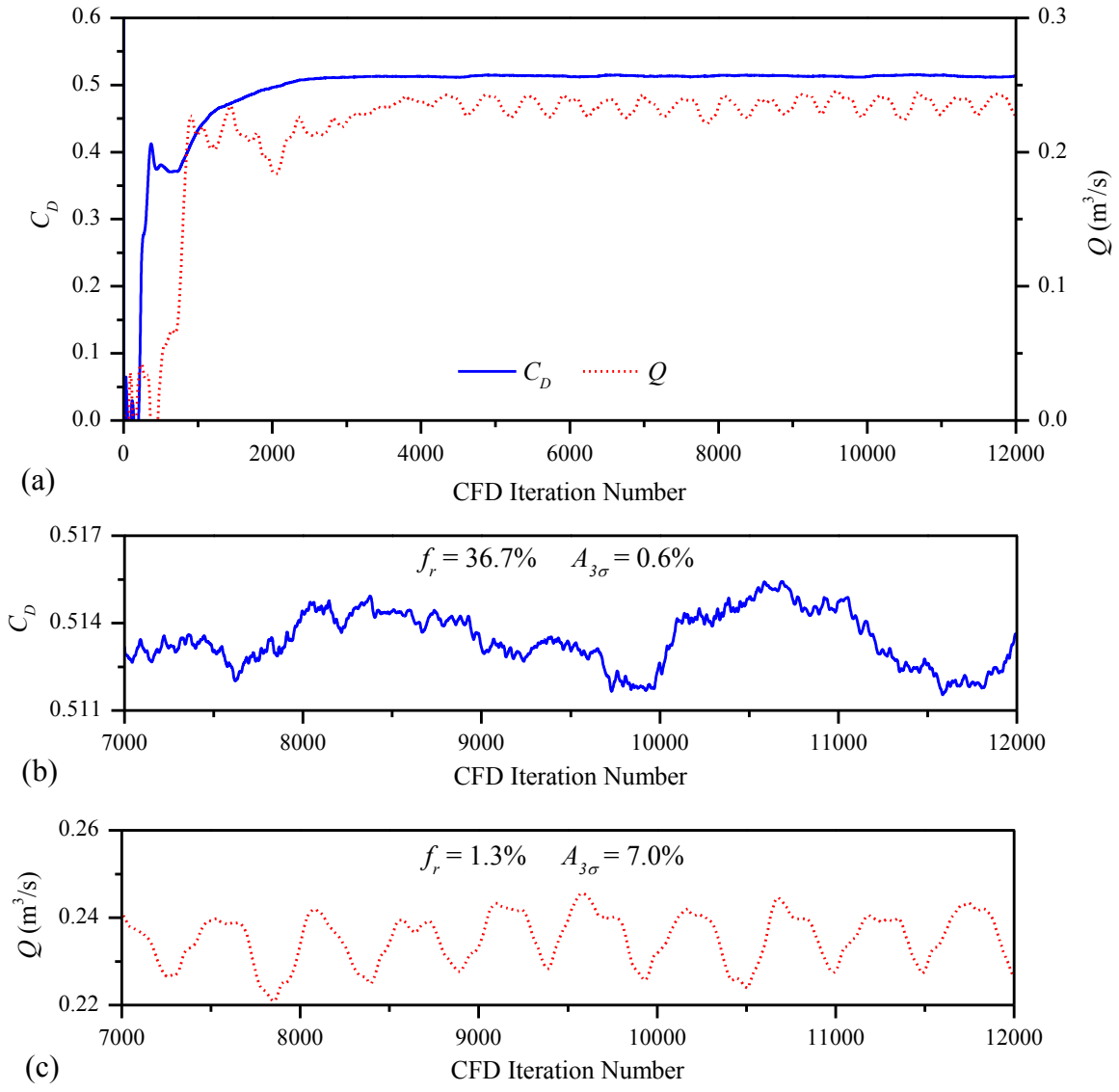

Figure 7: Plots of typical noise levels for one CFD solution.

In an effort to mask the noise levels, each solution was run for a further 2000 iterations (beyond the initial 10000) before taking an average of the quantity of interest over the extended portion. New metamodels were built using these 'mean value' solutions; however, this did not remedy the problems and optimization was not successful[40].

F. Revised problem

The fact that masking pronounced noise levels using mean solutions did not remedy optimization problems led to the conclusion that there was something fundamentally wrong with F_2. Whilst the ventilation rate is a suitable measure of the air quality within the trailer, its calculation is based on 2D surface integrals of the volumetric flow rate through each of the side vents in the lower deck (Figure 5). As these regions are oblique to the free-stream, large flow gradients are present and this leads to the high noise levels cited above. Further investigation revealed that the vent openings experiencing the greatest flow gradients produced the highest variability (and thus noise) from iteration to iteration as each solution progressed. By basing the objective function on a 3D volume-averaged quantity, the impact of high flow gradients reduces substantially. Consequently, the temperature humidity index (THI)[41], which has units of ºF, was chosen. By taking the volume-average of this quantity throughout the lower deck of the trailer, thermal comfort and thus animal welfare is considered instead of ventilation. Accordingly the problem was revised to:

$$\min F_1(\boldsymbol{d}) \text{ and } \min F_3(\boldsymbol{d}), \tag{6}$$

where F_3 is the objective function representing THI. Using the previous solutions as a basis, all simulations were run for an additional 4000 iterations with extra transport equations for energy and species also solved; these account for thermal effects and humidity which are required in the calculation of THI. Source terms for energy and moisture production were used to represent animal warmth and perspiration so that F_3 could be calculated for hot (30 ºC) and humid (relative humidity = 95%) ambient conditions (see ref 10 for more details).

Results from the revised simulations were found to be free of significant noise levels, with mean amplitudes of 0.3% and 0.2% evident for F_1 and F_3, respectively. Overall, the noise frequency is greater in the results for F_3; however, the small amplitudes present for both objective functions underline the dramatic improvement which is in complete contrast to the noisy responses seen earlier.

G. Optimum design

The aforementioned optimization strategy was repeated with the revised data. As expected the drag metamodel predicted the same optimum fairing design (i.e. for F_1) as before, whereas the THI metamodel revealed a candidate for min $F_3(\boldsymbol{d})$. An additional CFD simulation verified that this design gave the smallest THI of all the designs tested, suggesting that the optimum for F_3 had been found, see "Min-THI" in Fig. 8. This conclusion was verified from subsequent metamodel rebuilding and optimization with the additional point; it did not lead to a better design. Fig. 8 shows the final objective function plot which includes the minimum for each objective. Note that the small Pareto front was generated using a multi-objective genetic algorithm (MOGA)[42] which was applied to both metamodels.

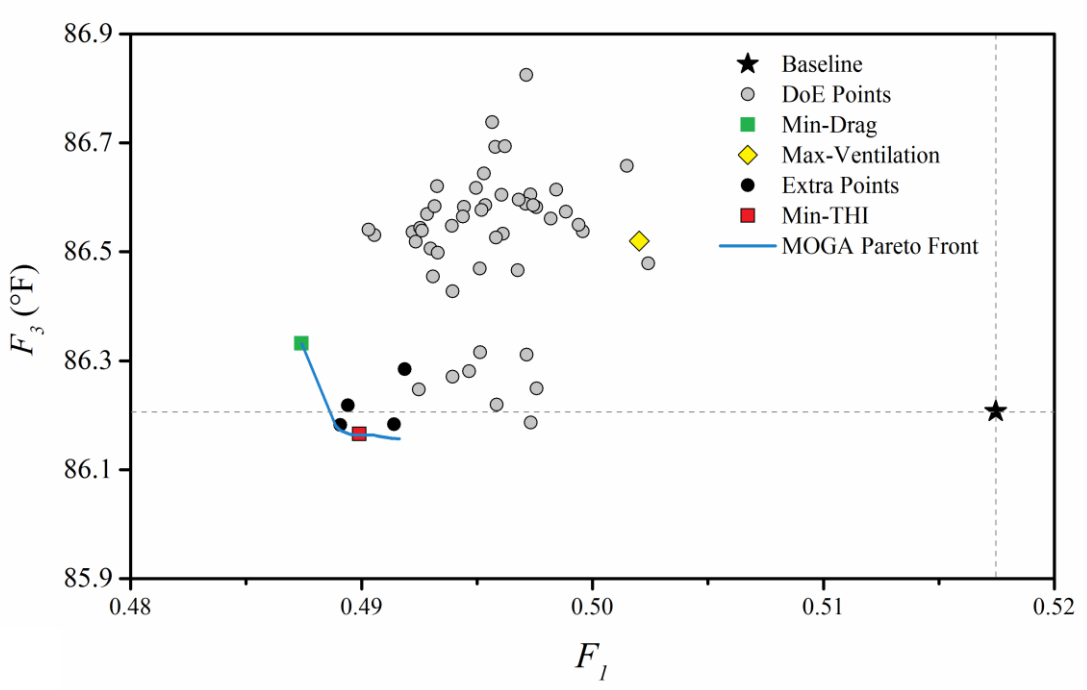

Figure 8: Objective function plot for the revised optimization problem

Of all the data points shown in Figure 8, the locations of the "Extra Points" are particularly noteworthy. These four designs were predicted in the isothermal optimization (section II part E) yet they exhibited sub-optimal performance in terms of ventilation and drag. With the above problem revision these very same designs now reside in the most promising region of the objective function landscape and one of them is in fact Pareto optimal. Therefore, in spite of the pronounced noise levels seen in the isothermal study, the MLS metamodelling technique was successful in filtering this noise and thus identifying optimal design characteristics. It follows that the MLS metamodels in this study were in fact more accurate than the high-fidelity CFD solutions used in the initial problem formulation. This stems from the inherent noise-handling capability of the approximation-based technique employed and is consistent with the earlier findings of Papila and Haftka[43].

Of all the designs considered, the "Min-THI" design was considered to be the overall optimum because it has the lowest value of THI whilst the corresponding drag is close to the minimum drag design. Fig. 9 illustrates the aerodynamic improvement by comparing the size of the wake of the optimum fairing to that of the baseline design (i.e. no fairing); the wake is significantly smaller and the overall drag is reduced by 5.3%.

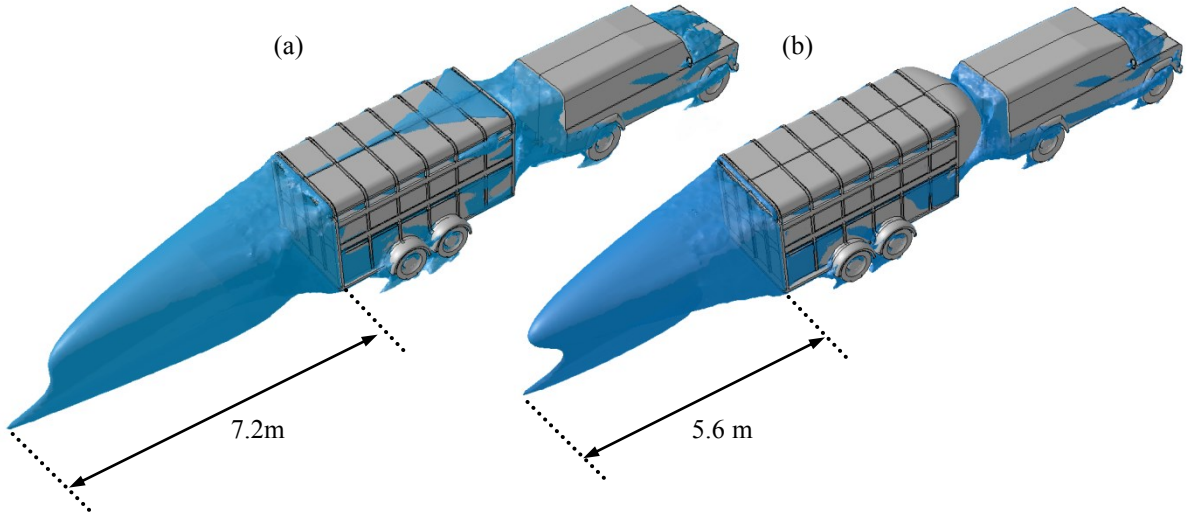

Figure 8: Wake structure comparison for (a) the baseline trailer and (b) the optimum one. Wake represented using iso-surfaces of constant velocity magnitude of 5 m/s.

IV. Discussion

The results presented in this article demonstrate how numerical noise can affect CFD solutions for road vehicle aerodynamics simulations. They illustrate how noise levels depend on the grid density, cell type and turbulence model which agrees with previous investigations[15-17]. Flow solutions computed on tetrahedral grid structures exhibit the greatest noise levels compared to those for hexahedral and polyhedral grids. On the whole, solutions obtained using the Spalart Allmaras turbulence model have far less noise than those for the realizable k-ε and SST k-ω models, for this particular application.

Noise levels are conveniently described in terms of the frequency and amplitude with variations in the latter effectively placing an error band on each solution. As steady-state solutions develop (beyond convergence), large amplitudes lead to iteration dependence and this can be particularly problematic when multiple designs are considered. A more representative solution for each design should be taken from the average of a suitably large sample using solution monitors; this serves to remove the fluctuations which make up numerical noise.

Although mean values are an effective way of masking noise levels, they cannot address fundamental problems with the choice of objective function. The livestock trailer optimization study undertaken illustrates how an inappropriate objective function can in fact prevent optimization. High flow gradients in critical locations within each flow field were responsible for pronounced noise levels and in searching for an optimum ventilation design a series of designs proposed by an MLS metamodel were shown to be ineffective. In spite of this, a subsequent change to the choice of objective function showed that these apparently sub-optimal designs resided in the most promising region of the objective function landscape (Fig. 7). The difference with the revised problem was that the objective function was based on a volume-averaged quantity which is far less susceptible to noise levels than 2D quantities measured in turbulent flow regions. Whilst it took the problem revision to identify an optimum design, the earlier MLS metamodels had in fact found optimal design characteristics despite noise levels in excess of 7%[40]. The conclusion that MLS approximations can deal with significant noise levels and still manage to identify optimum designs is a key point of this article.

In addition to the optimization strategy, the quality of the CFD methodology is equally important. Maximizing solution quality can be achieved by following verification and validation (V&V) procedures such as the widely adopted guidelines from the AIAA[44], ERCOFTAC[45] and ASME[46]. These advocate great care in preparing CFD simulations to minimise the errors present. The quality of CFD solutions can also be improved using experimental data which is useful for minimising uncertainties when prescribing boundary conditions for example. Although physical experiments are also subjected to errors, data obtained from them can be extremely valuable for validating the performance of individual numerical models.

V. Conclusion and Recommendations

Many steps can be taken to improve the chances of success in CFD-based optimization. It is essential to use high quality CFD responses which can be achieved by minimising errors where possible. Double-precision real number representation helps reduce round-off error, convergence errors can be avoided altogether if simulations are run for a sufficient number of iterations and grid independence studies can be used to select the most appropriate grid density and to provide an estimate of the discretization error. Validation data from relevant experiments is extremely valuable in ensuring that the fundamental flow physics is being adequately represented by the computations.

Whilst these steps are beneficial, the aforementioned errors contribute to fluctuations in a given solution which can be defined as numerical noise. Noise levels should be monitored for quantities of interest (i.e. objective functions) and the degree of variation observed. This study required simulations to be run for more than 2000 iterations (post convergence) to visualise both high and low frequency oscillations. Variation of up to 7% were seen and this had a negative impact. In the event of optimization problems in other investigations, it is advised, following ref 15, that a small region of the design space is explored to determine the sensitivity of the CFD responses to slight changes in the design variables. For a small enough region this procedure should result in almost linear variations; strong non-linearity (as was the case in Fig. 7) may be a sign of potentially destructive levels of numerical noise.

Emphasis should also be placed on the problem formulation and particularly on the choice of objective functions to be used in optimization studies. Basing these quantities on flow parameters which are measured in regions exhibiting high flow gradients can dramatically skew solutions. Where possible, such quantities should be based on solutions from a number of cells so that the average of these is representative of the objective function whilst retaining an element of stability (i.e. less noise). Finally, the benefits of approximation-based metamodels such as MLS are ideally suited to dealing with numerical noise and they can be readily incorporated into optimization studies.

Acknowledgements

The authors are thankful to Dr J. L. Summers, Dr G. J. Blyth and Mr T. Allwood for their time and commitment in ensuring the smooth running of computer hardware during the course of this work. The input of Professor J. Doherty is appreciated and the study would not have been possible without the financial support of the Department for the Environment, Food and Rural Affairs (DEFRA) under Grant Reference Number AW0933.

References

[1]Li, Y. and Nielsen, P.V. “Commemorating 20 Years of Indoor Air, CFD and Ventilation Research”, Indoor Air 2011, vol 21(6) pp. 442-453, 2011.

[2]Sun, H. and Lee, S. “Response Surface Approach to Aerodynamic Optimization Design of Helicopter Rotor Blade”, International Journal for Numerical Methods in Engineering; vol 64 pp. 125-142, 2011.

[3]Keane, A.J. and Nair, P.B. “Computational Approaches for Aerospace Design: The Pursuit of Excellence”, 1st Edition. John-Wiley and Sons, Chichester, England, 2005.

[4]Buscaglia, G., Auras, R.F. and Jai, M. “Optimization Tools in the Analysis of Micro-textured Lubricated Devices”, Inverse Problems in Science and Engineering, vol 14(4) pp. 635-378, 2006.

[5]Sienz, J., Bates, S.J. and Pittman, J.F.T. “Flow Restrictor Design for Extrusion Slit Dies for a Range of Materials: Simulation and Comparison of Optimization Techniques”, Finite Elements in Analysis and Design, vol 42 pp. 430-453 2006.

[6]Tahara Y, Tohyama S, Katsui T. CFD-Based Multi-Objective Optimization Method for Ship Design. International Journal for Numerical Methods in Fluids 2006; 52:499-527.

[7]Gilkeson, C.A., Toropov, V.V., Thompson, H.M., Wilson, M.C.T., Foxley, N.A. and Gaskell, P.H. “Aerodynamic Shape Optimization of a Low Drag Fairing for Small Livestock Trailers”, Proceedings of the 12th AIAA/ISSMO Multidisciplinary Analysis and Optimization Conference, Victoria, British Columbia, Canada, American Institute of Aeronautics and Astronautics. Paper No. 2008-5903, 2008.

[8]Krajnović S. "Optimization of Aerodynamic Properties of High-Speed Trains with CFD and Response Surface Models. The Aerodynamics of Heavy Vehicles II: Trucks, Buses, and Trains", Lecture Notes in Applied and Computational Mechanics, Springer, Berlin, pp. 197-211 2009.

[9]Gong, X., Gu, Z., Li, Z., Song, X. and Wang, Y. "Aerodynamic Shape Optimization of a Container-Truck's Wind Deflector Using Approximate model", Society of Automotive Engineering. Paper No. 2010-01-2035, 2010.

[10]Gilkeson, C.A., Toropov, V.V., Thompson, H.M., Wilson, M.C.T., Foxley, N.A. and Gaskell, P.H. "Multi-Objective Aerodynamic Shape Optimization of Small Livestock Trailers", Engineering Optimization, vol 45(11) pp. 1390-1330 2013.

[11]Khan, M.A.I., Noakes, C.J. and Toropov, V.V. "Development of a Numerical Optimization Approach to Ventilation System Design to Control Airborne Contaminant Dispersion and occupant Comfort", Building Simulation, vol 5 pp. 39-50 2012.

[12]Fan, J., Eves, J., Thompson, H.M., Toropov, V.V., Kapur, N., Copley, D. and Mincher, A. "Computational Fluid Dynamic Analysis and Design Optimization of Jet Pumps", Computers & Fluids, vol 46 pp. 212-217 2011.

[13]Giunta, A.A., Dudley, J.M., Narducci, R., Grossman, B., Haftka, R.T., Mason, W.H. and Watson, L.T. "Noisy Aerodynamic Response and Smooth Approximations in HSCT Design", Proceedings of the fifth AIAA/USAF/NASA/ISSMO Symposium on Multidisciplinary Analysis and Optimization, Panama City, Florida, pp. 1-12 1994.

[14]van Keulen, F., Haftka, R.T. and Qu, X-Y. "Noise and Discontinuity Issues in Response Surfaces Based on Functions and Derivatives", Proceedings of 41st AIAA/ASME/ASCE/AHS/ASC Structures, Structural Dynamics and Materials Conference, Atlanta, Georgia, USA, Paper No. AIAA-00-1363 2000.

[15]Madsen, J.I., Shyy, W. and Haftka, .RT. "Response Surface Techniques for Diffuser Shape Optimization", American Institute of Aeronautics and Astronautics Journal vol 38(9) pp. 1512-1518 2000.

[16]Shyy, W. Papila, N., Vaidyanathan, R. and Tucker, K. "Global Design Optimization for Aerodynamics and Rocket Propulsion Components", Progress in Aerospace Sciences, vol 37 pp. 59-118 2001.

[17]Burman, J. and Gebart, B.R. "Influence from Numerical Noise in the Objective Function for Flow Design Optimisation", International Journal of Numerical Methods for Heat & Fluid Flow, vol 11(1) pp. 6-19 2001.

[18]Forrester, A.I.J., Bressloff, N.W. and Keane, A.J. "Optimization Using Surrogate Models and Partially Converged Computational Fluid Dynamics Simulations", Proceedings of the Royal Society A, vol 462 pp. 2177-2204 2006.

[19]Forrester, A.I.J, Keane, A.J and Bressloff, N.W. "Design and Analysis of "Noisy" Computer Experiments", American Institute of Aeronautics and Astronautics Journal, vol 44(10) pp. 2331-2339 2006.

[20]Connor, J.J. and Wang, J.D. "Finite element modelling of hydrodynamic circulation", In: Numerical Methods in Fluid Dynamics. (Edited by Brebbia, C.A and Connor, J.J). Pentech Press, London, 1974.

[21]Wang, J.D. and Connor, J.J. "Mathematical Modelling of Near Coastal Circulation", MIT Parsons Laboratory Report No. 200, 1975.

[22]Gray, W.G. and Lynch, D.R. "On the Control of Noise in Finite Element Tidal Computations: A Semi-Implicit Approach", Computers & Fluids, vol 7 pp. 47-67 1979.

[23]Walters, R.A. "Numerically Induced Oscillations in Finite Element Approximations to the Shallow Water Equations", International Journal for Numerical Methods in Fluids, vol 3 pp. 591-604 1983.

[24]van Keulen, F. and Toropov, V.V. "Multipoint Approximations for Structural Optimization Problems with Noisy Response Functions", Proceedings of 1st ISSMO/NASA/AIAA Internet Conference on Approximations and Fast Reanalysis in Engineering Optimization. Published on a CD ROM by ISSMO/NASA/AIAA, 1998.

[25]Toropov, V.V. "Modelling and Approximation Strategies in Optimization – Global and Mid-Range Approximations, Response Surface Methods, Genetic Programming, Low/High Fidelity Models", In: Blachut J, Eschenauer HA (Eds.). Emerging Methods for Multidisciplinary Optimization, CISM International Centre for Mechanical Sciences, Springer Wien, New York, 2001.

[26]Ahmed, S.R., Ramm, G. and Faltin, G. "Some Salient Features of the Time-Averaged Ground Vehicle Wake", Society of Automotive Engineering. Paper No. 840300, 1984.

[27]Ansys Inc. http://ansys.com/products/fluid-dynamics, 2014. Accessed 25/06/2014.

[28]Gilkeson, C.A., Thompson, H.M., Wilson, M.C.T., Gaskell, P.H. and Barnard, R.H. "An Experimental and Computational Study of the Aerodynamic and Passive Ventilation Characteristics of Small Livestock Trailers", Journal of Wind Engineering and Industrial Aerodynamics, vol 97 pp. 415-425 2009.

[29]Gilkeson, C.A. "Analysis and Optimization of Ventilation and Drag in Small Livestock Trailers Using Computational Fluid Dynamics", PhD thesis. University of Leeds, 2009.

[30]Spalart, P.R. and Allmaras, S.A. "One-Equation Turbulence Model for Aerodynamic Flows", American Institute of Aeronautics and Astronautics Journal, Paper No. 92-0439, 1992.

[31]Shih, T-S., Liou, W.W., Shabbir, A., Yang, Z. and Zhu, J. "A New k-ε Eddy Viscosity Model for High Reynolds Number Flows", Computers & Fluids, vol 24(3) pp. 227-238 1995.

[32]Menter, F. "Two-equation Eddy-viscosity Turbulence Model for Engineering Applications", American Institute of Aeronautics and Astronautics Journal, vol 32 pp. 1598-1605 1994.

[33]Patankar, S.V. and Spalding, D.B. "A Calculation Procedure for Heat, Mass and Momentum Transfer in Three-Dimensional Parabolic Flows", International Journal of Heat and Mass Transfer, vol 15(10) pp. 1787-1806 1972.

[34]Narayanan, A., Toropov, V.V., Wood, A.S. and Campean, I.F. "Simultaneous Model Building and Validation with Uniform Designs of Experiments", Engineering Optimization, vol 39(5) pp. 497-512 2007.

[35]Audze, P. and Eglais, V. "New approach to planning out of experiments", Problems of Dynamics and Strength, Zinatne, Riga (in Russian), vol 35 pp. 104-107 1977.

[36]Rikards, R. "Elaboration of Optimal Design Models for Objects from Data of Experiments", In Pedersen P, ed., Optimal Design with Advanced Materials, The Frithiof Niordson Volume", Proceedings of the IUTAM Symposium, Lyngby, Denmark, pp. 149-162 1993.

[37]Choi, K.K., Youn, B.S. and Yang, R.J. "Moving Least Square Method for Reliability-Based Design Optimization. Proceedings of 4th World Congress of Structural and Multidisciplinary Optimization, Dalian, China, CD-ROM Proceedings, Liaoning Electronic Press (WCSMO-4), 2001.

[38]Toropov, V.V., Schramm, A., Sahai, A., Jones, R. and Zeguer, T. "Design Optimization and Stochastic Analysis Based on the Moving Least Squares Method. 6th World Congress of Structural and Multidisciplinary Optimization, Rio de Janeiro, Brazil, CD-ROM Proceedings, eds.: Herskovits, J., Mazorche, S., Canelas, A., COPPE Publication, Rio de Janeiro, 2005.

[39]HyperStudy, Altair Engineering Ltd, 2014, http://www.altairhyperworks.co.uk, accessed 20/06/2014.

[40]Gilkeson, C.A., Toropov, V.V., Thompson, H.M., Wilson, M.C.T., Foxley, N.A. and Gaskell, P.H. "Dealing With Numerical Noise in CFD-Based Design Optimization", Computers & Fluids, vol 94 pp. 84-97 2014.

[41]Dikmen, S. and Hansen, P.J. "Is the Temperature-Humidity Index the Best Indicator of Heat Stress in Lactating Dairy Cows in a Subtropical Environment?", Journal of Dairy Science, vol 92 pp. 109-116 2009.

[42]Fonseca, C.M. and Fleming, P.J. "An Overview of Evolutionary Algorithms in Multiobjective Optimization. Evolutionary Computation", vol 3 pp. 1-16 1995.

[43]Papila, M. and Haftka, R.T. "Response Surface Approximations: Noise, Error Repair, and Modeling Errors", American Institute of Aeronautics and Astronautics Journal, vol 38(12) pp. 2336- 2343 2000.

[44]Guide for the Verification and Validation of Computational Fluid Dynamics Simulations, American Institute of Aeronautics and Astronautics, Guide G-077-1998(2002), 2002.

[45]ERCOFTAC Special Interest Group on "Quality and Trust in Industrial CFD" Best Practice Guidelines Version 1.0. eds.: Casey M, Wintergerste T. European Research Community On Flow Turbulence and Combustion, 2000.

[46]Standard for Verification and Validation in Computational Fluid Dynamics and Heat Transfer, The American Society of Mechanical Engineers, ASME V&V 20-2009, 2009.